Opposite Patterns of Synchrony in Sympatric Disease Metapopulations

Pejman Rohani,* David J. D. Earn,† Bryan T. Grenfell

Measles epidemics in UK cities, which were regular and highly synchronous before vaccination, are known to have become irregular and spatially uncorrelated in the vaccine era. Whooping cough shows the reverse pattern, namely a shift from spatial incoherence and irregularity before vaccination to regular, synchronous epidemics afterward. Models show that these patterns can arise from disease-specific responses to dynamical noise. This analysis has implications for vaccination strategies and illustrates the power of comparative dynamical studies of sympatric metapopulations.

A central debate in ecology concerns the relative importance of deterministic and stochastic processes in shaping the dynamics of populations (*1*). This issue has become more complex since the recognition that patterns of population fluctuation are substantially influenced by spatial structure and synchrony (*2*). Progress has been made in studies showing close dynamical agreement between models and data (*3*, *4*), the exploration of spatial structure (*5*–*7*), and comparative analyses of population dynamics across species (*8*). However, models and long-term observed spatiotemporal data have not been combined to analyze the comparative contemporaneous dynamics of sympatric metapopulations. This can be achieved in the study of childhood bacterial and viral infections (for example, measles, whooping cough, rubella, and chicken pox), for which there are unusually extensive spatiotemporal data and realistic models (*6*, *9*, *10*).

We present an analysis of weekly incidence data from 60 cities in England and Wales from 1944 to 1994 for measles and whooping cough (*11*, *12*). The time series encompass dramatic changes in effective demographic parameters, particularly as a result of nationwide vaccination schemes (starting in 1968 for measles and 1957 for whooping cough). This permits the study of the comparative dynamical effects of vaccination as a "natural experiment." Apart from their broad ecological interest, understanding the mechanisms that drive the dynamics of disease metapopulations is also fundamental in the design of successful vaccination programs.

The two infections have a similar reproductive ratio (R_0) of 16 to 18 (*9*, *12*). The measles virus is transmitted by means of aerosol particles and is highly infectious. It conforms very closely to the assumptions of the SEIR (susceptible, exposed, infectious, recovered) class of models, with a latent period of about 8 days, an effective infectious period of about 5 days, and life-long immunity after infection (*9*). Before mass immunization, the dynamics of measles were highly synchronized across England and Wales with a pronounced 2-year period from

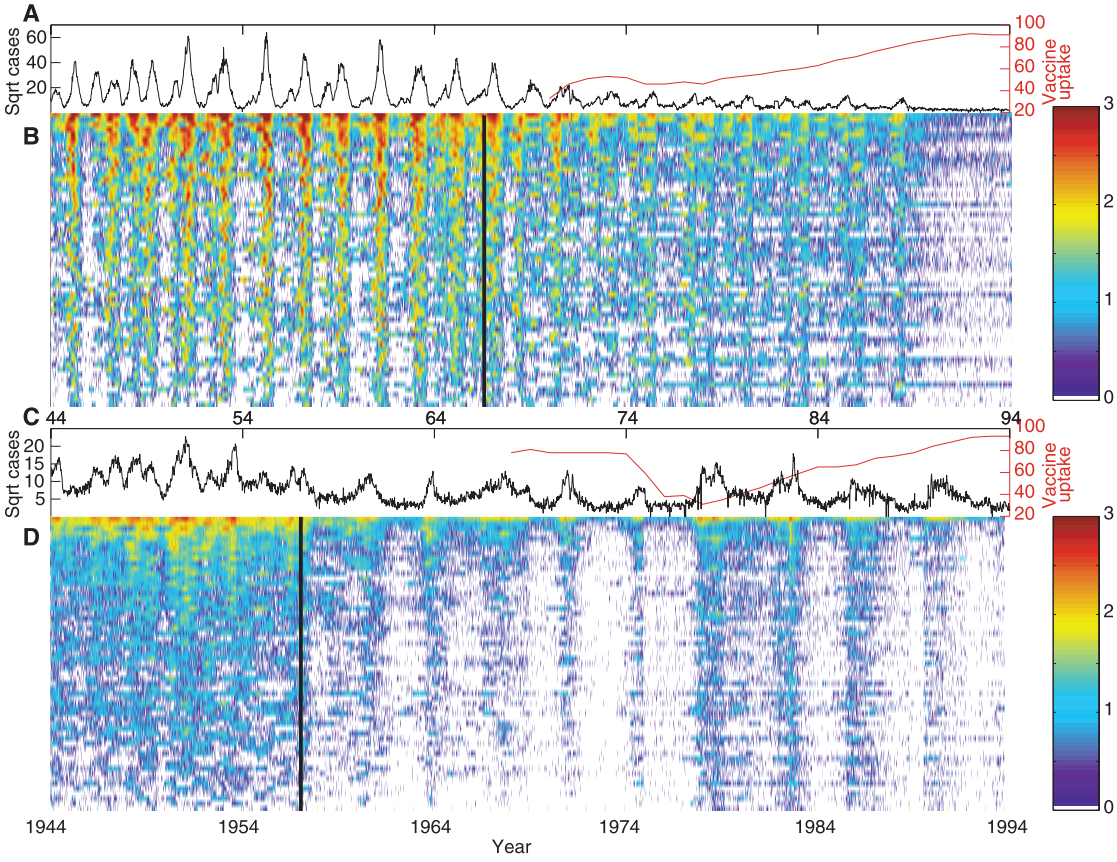

Fig. 1. Measles and whooping cough notifications in England and Wales from 1944 to 1994, obtained from the Registrar General's Weekly Returns. (**A**) Time series for measles in London (black line) together with the published vaccine uptake levels (percentage of infants vaccinated) for England and Wales (*20*), starting in 1968 (red line). (**B**) The spatial distribution of $\log_{10}$ (1 + measles cases) with cities arranged in descending order of population size (from top to bottom) and colors denoting epidemic intensity (white regions highlight periods with no reported cases). (**C**) Cases of whooping cough in London (black line), with the vaccine uptake levels (red line) (*20*). (**D**) The spatial data for pertussis in England and Wales with the same color scheme as in (B). In (D), there is a subtle but noticeable change in the pattern of case reports from 1974 to 1984. This was due to a nationwide scare concerning the safety of the pertussis vaccine, resulting in a dramatic drop in vaccine uptake levels (30% in 1978) (*20*). In addition to an increase in the reported cases of pertussis, the data suggest that this relatively sudden reduction in vaccine uptake caused a slight spatial desynchronization. The vertical black lines in (B) and (D) represent the onset of vaccination. Sqrt, square root.

1950 (Fig. 1, A and B) (*6*, *13*, *14*). In contrast, the dynamics of measles in the vaccine era show little temporal or spatial pattern, consisting of annual and 2- to 3-year fluctuations (*15*) that are spatially uncorrelated (*13*) (Fig. 1, A and B).

Whooping cough is a respiratory disease caused by the highly infectious bacterium *Bordetella pertussis*, with an average latent period of 8 days and an infectious period of 14 to 21 days (*16*–*18*). The immunological response to pertussis varies, with known instances of immunity waning after infection (*18*). Despite this potential complication, whooping cough dynamics are relatively well described by the SEIR formalism (*9*, *17*, *19*, *20*).

The spatiotemporal dynamics of whooping cough are dramatically different from those of measles. Figure 1, C and D, shows that, compared with measles, pertussis exhibits the reverse pattern of spatial synchrony, before and during the vaccine era. In the prevaccination era (1944–57), there is little spatial correlation in epidemics of whooping cough; each city exhibits bursts of about 2- to 2.5-year fluctuations, punctuated with periods of annual outbreaks. Mass vaccination in 1957, however, stimulated highly synchronized 3.5-year pertussis outbreaks across England and Wales. These spatial correlations are analyzed statistically in Fig. 2; compared with measles, the spatial dynamics of whooping cough do indeed show the opposite response to vaccination, with significantly higher correlations among communities in the vaccine era.

For measles, the predominantly biennial prevaccination pattern in large cities after 1950 is accurately reproduced by simple deterministic SEIR models with seasonally varying contact rates, as dictated by the pattern of school terms (*21*, *22*). Similar deterministic models of whooping cough have been unable to capture the observed outbreaks, both before and after the start of mass vaccination. We investigated whether the missing ingredient might be stochasticity and found that, in the absence of vaccination, an event-driven, seasonally forced Monte Carlo SEIR model (*12*, *22*) generated a mixture of 2- to 2.5-year and annual cycles, consistent with the observed time series (*22*). The multiannual cycles are stimulated by stochastic resonance around the annual deterministic attractor. The model also generates epidemics in the vaccine era that are very similar to the data, with a pronounced 3.5-year period (Fig. 3, C and D).

These findings are in agreement with Hethcote's study of pertussis case reports in the United States (*17*). Using a complex age-structured model that incorporated different levels of vaccine-induced and infection-induced immunity, Hethcote also concluded that stochasticity is needed if the observed multiannual oscillations are to be accurately captured.

A detailed analysis reveals that the deterministic whooping cough attractor is extremely sensitive to stochastic effects (*23*). Small perturbations can cause relatively long transient behavior that is qualitatively different from the asymptotic dynamics. This is in contrast with measles, where trajectories that are pushed away from the biennial attractor by noise return to it rapidly and these brief transients are themselves strongly biennial.

We would like to determine the biological mechanisms that underlie this contrast in the dynamics of measles and whooping cough. The most important differences between the two diseases lie in their epidemiological parameters: Whooping cough has an infectious period about three times as long as that of measles. The dynamics of measles, with its shorter infectious period, are strongly dictated by the pattern of seasonality, whereas the relatively brief periods of low contact rates between children when schools are out of term are likely to have a much less profound effect on a disease with a long duration of infection. Pertussis epidemics do appear much less locked into phase by seasonal forcing, although it is an important feature of the dynamics (*17*).

These differences in the interaction between nonlinearity, dynamical noise, and external forcing also account for the observed spatial patterns in the prevaccination and vaccine eras. The large-scale spatial coherence in prevaccination measles epidemics may be due to the presence of a unique (typically biennial) attractor at the individual city scale and epidemiological coupling, which transfers the infection to other centers and tends to push epidemics into phase. The vaccine era is more complicated. Elsewhere, we have demonstrated that vaccination moves model measles dynamics into a parameter region that may contain multiple stable solutions, with finely intertwined basins of attraction (*21*). In the presence of stochasticity, trajectories in different cities might switch between attractors in a complex manner, resulting in spatial asynchrony of epidemics. A fully stochastic SEIR model captures the qualitative

Department of Zoology, University of Cambridge, Downing Street, Cambridge CB2 3EJ, UK.

*To whom correspondence should be addressed. E-mail: pej@zoo.cam.ac.uk

†Current address: Department of Mathematics and Statistics, McMaster University, 1280 Main Street West, Hamilton, Ontario, Canada L8S 4K1.

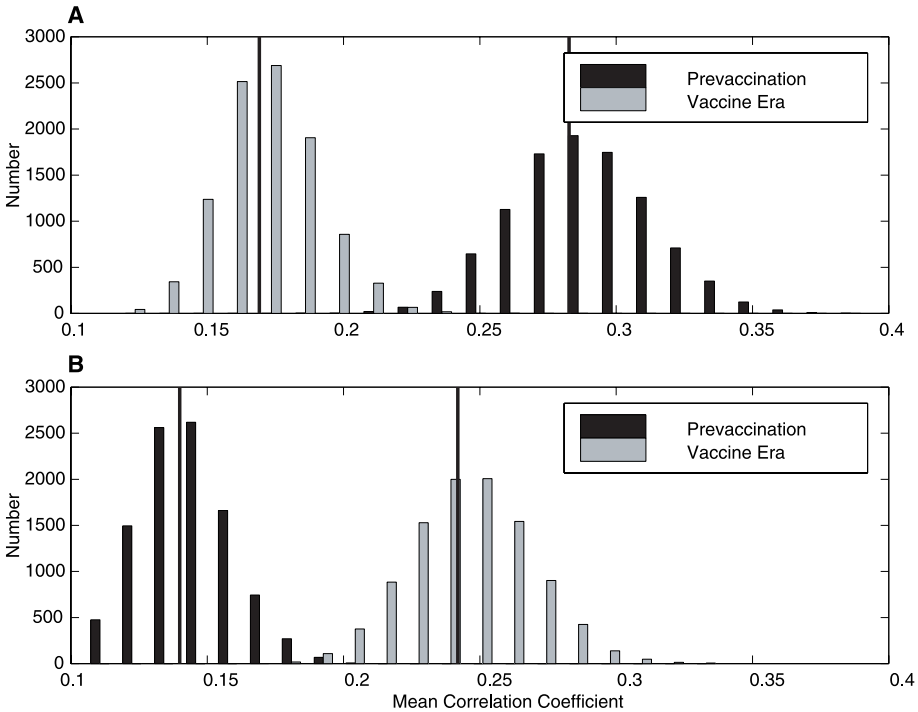

Fig. 2. Frequency histograms contrasting the spatial correlation for measles (**A**) and whooping cough (**B**) before and after the start of vaccination in England and Wales. For pertussis, we contrasted the prevaccine period 1944–57 with 1957–74; the comparable periods for measles are 1944–68 and 1968–88. We estimated the 60 × 60 matrix of Pearson correlations between cities and calculated the mean of the lower triangle. We then established whether the means before and after vaccination are significantly different by bootstrapping the entries of the correlation matrix (*7*). The values depicted represent the mean correlation of 10,000 bootstraps, with the solid line showing the England and Wales means. This illustrates that the spatial synchrony of measles and pertussis is changed by vaccination and is in the opposite direction. The mean correlation coefficients for measles in the prevaccination and the vaccination era are 0.29 (bootstrap 95% confidence interval = {0.24, 0.34}) and 0.17 {0.14, 0.21}, respectively. The corresponding mean correlation coefficients for whooping cough are 0.14 {0.11, 0.18} and 0.25 {0.20, 0.29}, respectively.

dynamics of measles in the vaccine era (Fig. 3, A and B).

The absence of spatial synchrony in the prevaccine pertussis data is not surprising, given the more crucial roles that stochasticity and transients play in determining its dynamics and the weaker phase-locking with seasonality (Fig. 1D). We would like to determine why whooping cough outbreaks become so highly synchronized with a period of 3.5 years in the vaccine era. There are probably several factors responsible for this transition. First, vaccination increases the mean age at infection, which in turn increases the natural period of the system, giving rise to coherent 3.5-year cycles (*9*, *24*). Second, in the presence of this unique dynamical attractor, a concerted nationwide vaccination effort starting in 1957 is likely to have acted as a strong synchronized "shock" to the system, forcing different communities into phase. We explored these two factors using a stochastic SEIR model for 10 coupled populations, with vaccination starting at year 100. Despite its simplicity, the model accurately captures the qualitative effects of vaccination on spatial synchrony (Fig. 3, C and D). The spatially synchronized initiation of vaccination drives the model dynamics to 3.5-year cycles, with a lower effective R_0 (*24*).

The increase in the mean age at infection in the vaccine era might also result in greater amounts of movement in the infected population, thus increasing epidemiological coupling. We would expect this to enhance epidemic synchronization (when there is a unique attractor).

Our findings have implications for vaccination strategies and metapopulation dynamics. Since the influential work of Fine and Clarkson (*25*), it has been thought that although pertussis vaccination reduced the total number of new cases, it did not lengthen the period between whooping cough outbreaks. The general consensus, therefore, has been that moderate levels of immunization cannot disrupt the transmission of pertussis, although it prevents disease (*18*, *20*). The post-1957 region of Fig. 1D shows, however, that vaccination had two major effects on pertussis epidemics: (i) Their period markedly increased from at most 2.5 years to 3.5 years, and (ii) they became highly synchronized, with very deep troughs between outbreaks. These dynamical transitions as a result of pertussis vaccination suggest that immunization is having a pronounced effect on the circulation of the infection.

Another implication of this work concerns the use of vaccination pulsed across all ages. This alternative immunization strategy has been proposed in an important body of theoretical work (*26*) and has gained much popularity, mainly for economic and logistic reasons. Superimposing pulses on continuous vaccination may also provide a spatial benefit by synchronizing local fade-outs, thus increasing the likelihood of global eradication (*6*, *14*). This is potentially a useful effect for measles, for which vaccination had a spatially decorrelating effect (*13*). However, our findings indicate that the spatial consequences of pulsed vaccination are more difficult to predict for pertussis, for which continuous vaccination alone has synchronized outbreaks. In particular, our results suggest that dynamical factors need to be taken into account: The timing of any pulses should avoid disturbing both the deep troughs and the long interepidemic period currently observed.

This work also demonstrates the ecological benefits of studying comparative spatiotemporal dynamics in sympatric disease metapopulations. An intricate balance between stochasticity, seasonality, and nonlinearity makes a profound difference for the dynamics of two childhood infections, in the same host metapopulation, with largely the same dispersal patterns and the same pattern of seasonal forcing. The prevaccine dynamics of measles in large UK cities are relatively well explained with a deterministic model; in contrast, prevaccine pertussis dynamics exhibit a subtle interaction between noise and determinism (*4*, *27*) and cannot be modeled adequately without stochasticity. The scenario is reversed in the vaccine era, during which measles appears to be highly influenced by stochasticity and pertussis outbreaks can be explained with simple, deterministic arguments (*24*). Childhood diseases are likely to prove excellent systems for further investigation of these issues.

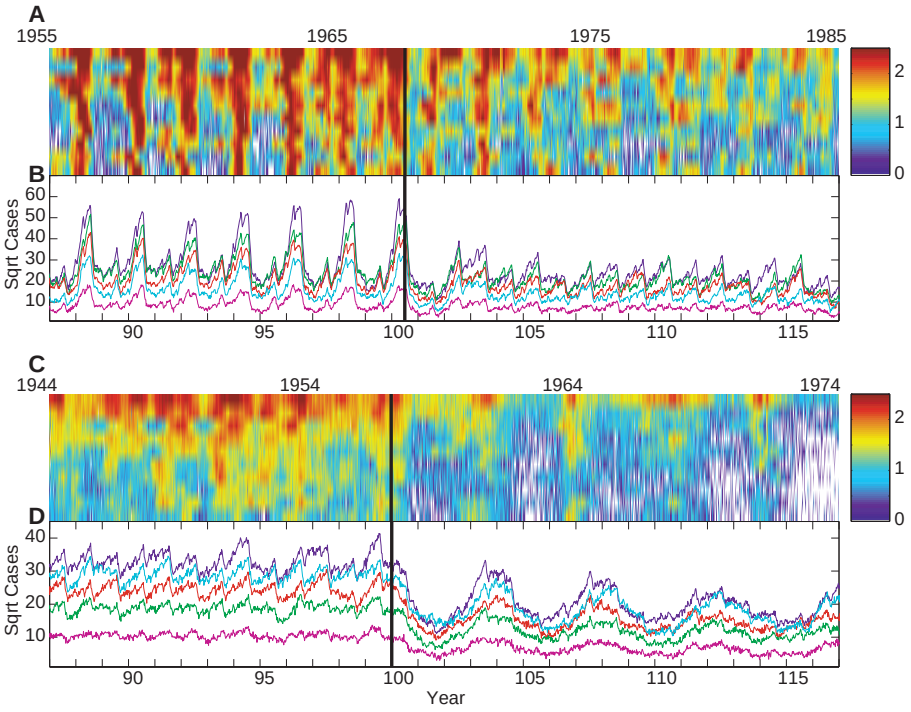

Fig. 3. Spatiotemporal data for measles (**A**) and whooping cough (**C**) (color scale is as in Fig. 1) in the largest 10 cities in England and Wales, compared with time-series data from the stochastic spatially structured simulation model (**B** and **D**) [10 populations with sizes evenly distributed in the range (3×10^5, 3×10^6) were used in the simulation, but only five populations are shown in the figure]. For details of the model, see (*22*). In (B), the model focuses on the dynamics of measles in the prevaccine era, showing highly synchronized biennial outbreaks, which give way to complex and less correlated epidemics after the introduction of vaccination at year 100.5 [as demonstrated by Aron (*28*), the precise effects of vaccination are subtly sensitive to the time of year when vaccination is introduced]. In (D), the analogous model results for whooping cough in 10 large cities before vaccination exhibit 2- to 2.5-year fluctuations with a pronounced annual component and little spatial synchrony. These dynamics give way to highly correlated 3.5-year epidemics after vaccination starting in year 100. We used the published vaccine uptake levels described by Miller and Gay (*20*). For pertussis, these data start in 1968; hence, we assumed a 60% initial vaccine uptake level increasing linearly to 78% in 1968 with 80% efficacy. Model parameters for pertussis were $1/\gamma = 14.0$ days, $1/\sigma = 8.0$ days, $\xi = 0.05$, and $b_1 = 0.15$. For measles, we used $1/\gamma = 5.0$ days, $1/\sigma = 8.0$ days, $\xi = 0.05$, and $b_1 = 0.25$.

Notes and References

1. R. M. May, *Science* **186**, 645 (1974); T. Royama, *Analytical Population Dynamics* (Chapman and Hall, London, 1992); C. Zimmer, *Science* **284**, 83 (1999).
2. R. Levins, *Bull. Entomol. Soc. Am.* **15**, 237 (1969); J. H. Brown and A. Kodric-Brown, *Ecology* **58**, 445 (1977).
3. R. F. Costantino, R. A. Desharnais, J. M. Cushing, B. Dennis, *Science* **275**, 389 (1997); M. J. Keeling and B. T. Grenfell, *Science* **275**, 65 (1997).
4. B. T. Grenfell *et al.*, *Nature* **394**, 674 (1998); K. Higgins, A. Hastings, J. N. Sarvela, L. W. Botsford, *Science* **276**, 1431 (1997).
5. M. P. Hassell, H. N. Comins, R. M. May, *Nature* **353**, 255 (1991); S. A. Levin, B. T. Grenfell, A. Hastings,

A. S. Perelson, *Science* **275**, 334 (1997); D. Grünbaum, *Am. Nat.* **151**, 97 (1998); I. Hanski, *Nature* **396**, 41 (1998); J. Swinton, J. Harwood, B. T. Grenfell, C. A. Gilligan, *J. Anim. Ecol.* **67**, 56 (1998).
6. B. T. Grenfell and J. Harwood, *Trends Ecol. Evol.* **12**, 395 (1997).
7. O. N. Bjørnstad, N. C. Stenseth, T. Saitoh, *Ecology* **80**, 622 (1999).
8. M. P. Hassell, J. H. Lawton, R. M. May, *J. Anim. Ecol.* **46**, 249 (1976); G. Sugihara and R. M. May, *Nature* **344**, 734 (1990); S. P. Ellner and P. Turchin, *Am. Nat.* **145**, 343 (1995).
9. R. M. Anderson and R. M. May, *Infectious Diseases of Humans* (Oxford Univ. Press, Oxford, 1991).
10. B. T. Grenfell and B. M. Bolker, *Ecol. Lett.* **1**, 63 (1998); D. Schenzle, *IMA (Inst. Math. Appl.) J. Math. Appl. Med. Biol.* **1**, 169 (1984).
11. The weekly case reports of measles and whooping cough are published in the Registrar General's Weekly Returns. These data have been estimated to represent about 50 to 60% of the actual cases for measles and 5 to 25% for whooping cough [J. A. Clarkson and P. E. M. Fine, *Int. J. Epidemiol.* **14**, 153 (1985)]. Although notification efficiency may affect the magnitudes of case reports, it will not create or alter the large-scale spatiotemporal trends observed in these data. Further, previous work has demonstrated very strong correlation between notified case reports, serological isolations of, for example, *B. pertussis* by the Public Health Laboratory Service, and independent notifications provided by the Royal College of General Practitioners General Practice Research Unit [(*25*); E. Miller, J. E. Vurdien, J. M. White, *Communicable Dis. Rep.* **2**, R152 (1992)].
12. P. Rohani, D. J. D. Earn, B. F. Finkenstädt, B. T. Grenfell, *Proc. R. Soc. London Ser. B Biol. Sci.* **265**, 2033 (1998).
13. B. M. Bolker and B. T. Grenfell, *Proc. Natl. Acad. Sci. U.S.A.* **93**, 12648 (1996).
14. D. J. D. Earn, P. Rohani, B. T. Grenfell, *Proc. R. Soc. London Ser. B Biol. Sci.* **265**, 7 (1998).
15. B. T. Grenfell, in *Chaos from Real Data: The Analysis of Nonlinear Dynamics in Short Ecological Time Series*, J. N. Perry and R. A. Smith, Eds. (Academic Press, San Diego, CA, 1999).
16. The infectious period for whooping cough consists of two characteristically very distinct phases: a catarrhal phase (symptoms include a mild fever and a cough), which lasts about 2 weeks, and the paroxysmal phase (intense bouts of coughing punctuated by the "whoop"). A case would be successfully diagnosed as pertussis at the start of the whooping phase, and, hence, for epidemiological purposes, the infectious period effectively lasts 14 days (assuming susceptibles in the family would have been infected by this time). Our results are not qualitatively affected by this assumption.
17. H. W. Hethcote, *Math. Biosci.* **145**, 89 (1997); *Can. Appl. Math. Q.* **6**, 61 (1998).
18. P. T. Scott, J. B. Clark, W. F. Miser, *Am. Fam. Phys.* **56**, 1121 (1997); J. D. Cherry, *Ann. Intern. Med.* **128**, 64 (1998).
19. B. T. Grenfell and R. M. Anderson, *Proc. R. Soc. London Ser. B Biol. Sci.* **236**, 213 (1989).
20. E. Miller and N. J. Gay, *Dev. Biol. Stand.* **89**, 15 (1997).
21. D. J. D. Earn, P. Rohani, B. M. Bolker, B. T. Grenfell, in preparation.
22. The spatially structured, deterministic SEIR equations for population i are given by

$$\frac{dS_i}{dt} = \mu N_i - (\lambda_i + \mu)S_i$$

$$\frac{dE_i}{dt} = \lambda_i S_i - (\mu + \sigma)E_i$$

$$\frac{dI_i}{dt} = \sigma E_i - (\mu + \gamma)I_i$$

$$\frac{dR_i}{dt} = \gamma I_i - \mu R_i$$

where $1/\sigma$ and $1/\gamma$ are the incubation and infectious periods, respectively, μ gives the per capita birth and death rates, and t is time. The force of infection is spatially structured and given by $\lambda_i = \beta(t)(I_i + \xi/n \Sigma_{j \neq i} I_j)/N_i$, where $\beta(t)$ represents the contact rate, ξ denotes the strength of epidemiological coupling, and N_i is the (constant) population size in patch i. Term-time forcing is implemented by making $\beta(t) = b_0 \times (1 + b_1)$ on school days and $\beta(t) = b_0 \times (1 - b_1)$ otherwise (b_0 is the basic contact rate, and b_1 denotes the amplitude of seasonality). Vaccination is incorporated by replacing the birth term by $\mu(1 - p)N_i$, where p is the proportion vaccinated. The analogous stochastic model assumes the same intrinsic processes as the above equations but is event driven [M. S. Bartlett, *J. R. Stat. Soc.* **120**, 48 (1957); B. T. Grenfell, *J. R. Stat. Soc. B* **54**, 383 (1992); B. T. Grenfell, B. M. Bolker, A. Kletczkowski, *Proc. R. Soc. London Ser. B Biol. Sci.* **259**, 97 (1995)]. We first estimated a time to the next event (δt) by calculating the sum of the frequencies of all possible events ($\eta = \Sigma_i [2 \times \mu N_i + \lambda_i S_i + \sigma E_i + \gamma I_i]$) and setting $\delta t = -\log(U_1)/\eta$, where U_1 is a uniform deviate in [0,1]. Next, we ordered all possible events as an increasing fraction of η and generated another uniform deviate ($U_2 \in [0,1]$) to obtain the nature of the next event. For example, if the uniform deviate is in the interval $[0,\mu N_1/\eta]$, then the event is a birth in population 1 ($S_1 \rightarrow S_1 + 1$, $N_1 \rightarrow N_1 + 1$), whereas if U_2 lies in $(\mu N_1/\eta, \lambda_1 S_1/\eta]$, then the next event is an infection in population 1 ($S_1 \rightarrow S_1 - 1$, $E_1 \rightarrow E_1 + 1$).
23. Environmental and demographic noise have little impact on the prevaccination biennial pattern of measles outbreaks, whereas they affect pertussis dynamics markedly (P. Rohani, M. J. Keeling, B. T. Grenfell, in preparation). This is caused by the differences in the local stability properties over the deterministic attractor for the two infections.
24. For the unforced SEIR system, the natural (damping) period of oscillations is $T \approx 2\pi\sqrt{AD}$, where A is the mean age at infection and D is the sum of infectious and incubation periods (*9*). For whooping cough before vaccination, the mean age at infection is 2 to 5 years and $D = 0.055$ years, giving a natural period of between 2.08 and 3.2 years. After vaccination, A would have risen to 5 to 7 years, giving a natural period of between 3.3 and 4.1 years. In (unforced) models with demographic or environmental stochasticity, resonance ensures that these oscillations are sustained, giving outbreaks with period T (assuming the population size is sufficiently large to avoid extinction of the pathogen) (*9*).
25. P. E. Fine and J. A. Clarkson, *Lancet* **1**, 666 (1982).
26. Z. Agur, L. Cojocaru, G. Mazor, R. M. Anderson, Y. L. Danon, *Proc. Natl. Acad. Sci. U.S.A.* **90**, 11698 (1993); D. J. Nokes and J. Swinton, *IMA (Inst. Appl. Math.) J. Math. Appl. Med. Biol.* **12**, 29 (1997); B. Shulgin, L. Stone, Z. Agur, *Bull. Math. Biol.* **60**, 1123 (1998).
27. O. N. Bjørnstad *et al.*, *J. Anim. Ecol.* **67**, 110 (1998).
28. J. L. Aron, *Theor. Popul. Biol.* **38**, 58 (1990).
29. We thank O. Bjørnstad, B. Bolker, B. Finkenstädt, R. Hamilton, M. Keeling, J. Swinton, and two anonymous reviewers for comments on this paper. P.R. was supported by a Natural Environment Research Council Postdoctoral Research Fellowship. D.J.D.E. was supported by a Wellcome Trust Postdoctoral Research Fellowship in Mathematical Biology. B.T.G. is supported by the Wellcome Trust.

22 April 1999; accepted 14 September 1999

Small Molecule Inhibitor of Mitotic Spindle Bipolarity Identified in a Phenotype-Based Screen

Thomas U. Mayer,[1]* Tarun M. Kapoor,[1] Stephen J. Haggarty,[2,3] Randall W. King,[2] Stuart L. Schreiber,[2,3] Timothy J. Mitchison[1,2]

Small molecules that perturb specific protein functions are valuable tools for dissecting complex processes in mammalian cells. A combination of two phenotype-based screens, one based on a specific posttranslational modification, the other visualizing microtubules and chromatin, was used to identify compounds that affect mitosis. One compound, here named monastrol, arrested mammalian cells in mitosis with monopolar spindles. In vitro, monastrol specifically inhibited the motility of the mitotic kinesin Eg5, a motor protein required for spindle bipolarity. All previously known small molecules that specifically affect the mitotic machinery target tubulin. Monastrol will therefore be a particularly useful tool for studying mitotic mechanisms.

Cell-permeable small molecules can rapidly perturb the function of their targets and are therefore powerful tools to dissect dynamic cellular processes. However, such modulators are not available for most of the proteins involved in essential processes, and many of the ones that are available are nonspecific. The only known small molecules that specifically affect the mitotic machinery target tubulin (*1*), a subunit of the microtubules in the mitotic spindle. To identify cell-permeable small molecules that target other mitotic proteins, we developed the screening strategy in (Fig. 1A). First, we used the versatile whole-cell immunodetection (cytoblot) assay (*2*) to identify compounds that increase the phosphorylation of nucleolin. Nucleolin is a nucle-

[1]Department of Cell Biology, and [2]Institute of Chemistry and Cell Biology, Harvard Medical School, Boston, MA 02115, USA. [3]Howard Hughes Medical Institute, Department of Chemistry and Chemical Biology, and Department of Molecular and Cellular Biology, Harvard University, Cambridge, MA 02138, USA.

*To whom correspondence should be addressed. E-mail: Thomas_Mayer@hms.harvard.edu